Artificial Intelligence-based Surrogate Model for Computation of the Electric Field of a High Voltage Transmission Line Ceramic Insulator with Corona Ring

Shahin Alipour Bonab, Alireza Sadeghi, and Mohammad Yazdani-Asrami*

Propulsion, Electrification & Superconductivity group, James Watt School of Engineering, University of Glasgow, Glasgow, G12 8QQ, United Kingdom

***Corresponding author's email: mohammad.yazdani-asrami@glasgow.ac.uk**

Abstract

Purpose - The ionization of the air surrounding the phase conductor in high-voltage transmission lines results in a phenomenon known as the Corona effect. To avoid this, Corona rings are used to dampen the electric field imposed on the insulator. The aim of this study is to present a fast and intelligent surrogate model for determination of the electric field imposed on the surface of a 120 kV composite insulator, in presence of the Corona ring.

Design/methodology/approach - Usually, the structural design parameters of the Corona ring are selected through an optimization procedure combined with some numerical simulations such as Finite Element Method (FEM). These methods are slow and computationally expensive and thus, extremely reducing the speed of optimization problems. In this paper, a novel surrogate model was proposed that could calculate the maximum electric field imposed on a ceramic insulator in a 120 kV line. The surrogate model was created based on the different scenarios of height, radius, and inner radius of the Corona ring, as the inputs of the model while the maximum electric field on the body of the insulator was considered as the output.

Findings - The proposed model was based on artificial intelligence techniques that have high accuracy and low computational time. Three methods were used here to develop the AI-based surrogate model, namely, Cascade Forward Neural Network (CFNN), Support Vector Regression (SVR), and K-Nearest Neighbors Regression (KNNR). The results indicated that the CFNN has the highest accuracy among these methods with 99.81% R-squared and only 0.045468 Root Mean Squared Error while the testing time is less than 10 ms.

Originality/Value – For the first time, a surrogate method is proposed for the prediction of the maximum electric field imposed on the high voltage insulators in the presence Corona ring which is faster than any conventional Finite Element Method (FEM).

Keywords- Corona ring, Electric field, Finite element method, Neural Networks, Surrogate model.

Paper type – Research paper

1. Introduction

Given the growing population of the world and the general trends towards electrification because of curbing global warming, electric power started to become the main source of energy. Therefore, delivering uninterruptable electrical energy has become a challenge and a massive investment point during the last decade. Some challenges are endangering the safe, reliable, and uninterrupted electrical power delivery to the end customers. Among them, high amounts of energy transmission loss, transients, and short-circuit faults are critically important. Many of these challenges originate in the transmission section of the power grid (Seyyedbarzegar, et al, 2015b; Alipour Bonab, et al, 2023). In this section, usually, the long overhead lines with high voltage are used to transmit the electrical energy from power plants or renewable energy resources to distribution systems. Again, in distribution systems, medium voltage lines are used to distribute the electrical energy to end users (Khodsuz, et al, 2015; Khodsuz, 2022). In the structure of these transmission/distribution lines, insulators are used to avoid any connection between phase wires and the body of the overhead lines tower (M.M Abravesh, 2016; Seyyedbarzegar et al, 2021). In high voltage lines and some medium voltage ones, a phenomenon happens which is called the Corona effect. This happens because of the ionization of the air around the high-voltage line conductor. The unideal air easily

ionizes and thus, it can conduct the electrical potential to the insulator, generate of a faint glow, create hissing noises, and causes the energy loss.

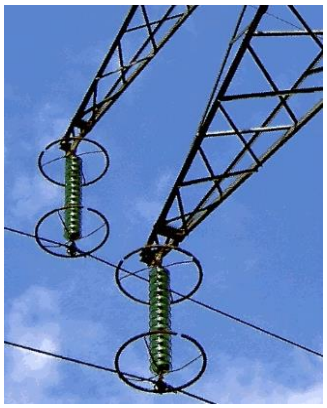

Figure 1. Insulator strings supporting a 225 kV power transmission line, France. The metal rings around the top and bottom of the insulators are called corona rings. They serve to reduce the potential gradient at sharp points to prevent corona discharge, and a leakage of current into the air (Corona ring).

This happens by induction of an electrical field on the body of the insulator which could cause a lifetime reduction of the insulators, decrease the insulator performance, reduce the reliability of the system, and increase the non-environmentally friendly noises. To avoid this, the solution that is proposed by electrical engineers, known as the Corona ring (Ilhan, Ozdemir, et al, 2015). Indeed, the Corona ring is used to redistribute the electrical field imposed on the insulator by being directly connected to the phase wire. In other words, Corona ring is used to modify the electric field, especially in sharp edges and points, grading the electric field by altering it on the surface of the insulator, and finally, reduce its intensity. For this purpose, Corona rings need to be installed at a specific distance from the body of insulator, with a pre-designed radius and inner tube radius (Salhi *et al.*, 2023). As shown in Figure 1, as an example of a Corona ring for high voltage lines, the Corona ring has a specific structural property; in other terms, it should be of a specific height, has a specific radius, and a specific tube radius.

The design procedure of the Corona ring is usually performed by parallelizing the optimization problem with the modelling procedure of the Corona ring and the insulator. Optimization procedure could be conducted through mathematical and intelligent optimization algorithms while Finite Element Method (FEM) is the most common type of modelling the structure of the insulator and Corona ring (Seyyedbarzegar, et al, 2015a). Among the papers, in literature, references (Diaz-Acevedo, et al, 2021; Zhang, 2021; Halloum, et al, 2022; M'Hamdi et al., 2022; Waghmare, et al, 2022) have used PSO for optimization, (Jiang et al., 2018; Aramugam, Illias, et al, 2019; Archana, et al, 2021; Khajavi, et al, 2023) have used GA for this purpose, and (Alti, et al, 2021; Illias et al., 2021) have used other intelligent methods for designing the Corona ring. Optimization is an iterative procedure where in each iteration, the objective function is evaluated until the stoppage criteria is met. In this regard and for the sake of Corona ring optimization, FEM-based models must be evaluated in each iteration. Although FEM-based models have high accuracy, their simulation time is high and could end up with a long design time that requires powerful computational resources. Recently, novel modelling methods have been used also to characterize the electrical behavior of insulators and Corona rings. In (Shi et al, 2019), a faster FEM model based on the indirect boundary integral equation of the electrostatic field and the Galerkin curved boundary element method is used to model the insulators in the presence of a Corona ring. In (Hanyu Ye, et al, 2015) a novel model is proposed that uses the co-Kriging method for dimension reduction of a 3D model to a 2D model. In (Bo Zhang *et al.*, 2006), a method based on the boundary element method and charge simulation method has been used to model the insulators and Corona ring. Also, recently, machine learning and deep learning methods have been used to characterize the different behavior of high voltage insulators. In (Aydogmus, 2009), Artificial Neural Network (ANN) has been used to estimate the electric field of 12 kV and 35 kV insulators, regarding their leakage distance. However, since the insulators are in medium voltage range, no Corona ring is considered in this study. In (Maraaba, et al, 2014; Maraabaet al, 2018), ANN is used to estimate the level of contamination in HV porcelain and glass insulators. Fuzzy logic and ANN have been used in (Bourek, et al, 2018) for prediction of flashover voltage in 250 kV insulators without considering the impact of Corona ring. Also, in (Niazi *et al.*, 2020), multiple machine learning methods is used to predict the critical flashover voltage of the HV insulators, in presence of humidity, pollution, and contamination. Failure of insulators by using support vector machine and ANN is conducted in (Medeiros *et al.*, 2022). Although much research has been conducted to increase the accuracy and the computational time of Corona rings and insulators, as well as the utilization of machine learning for characterizing the behavior of insulators, there is still a gap for very fast models with higher accuracy that can estimate the electric field of a HV insulator in presence of the Corona ring.

In this paper, a fast surrogate model based on artificial intelligence (AI) is proposed to compute the electrical field of the ceramic insulator during the design procedure

of the Corona ring. The surrogate model makes a direct connection between the input (variables) and output (final solution) of the problem, instead of solving the problem using the partial differential equations governing the domain of the problem. In this paper, two kinds of ANN have been used to make a mathematical connection between inputs of the model and the results, namely Feed Forward Neural Network (FFNN) and Cascade Forward Neural Network (CFNN). For this purpose, a series of simulation scenarios based on the characterization of a 120 kV ceramic insulator with Corona have been conducted, to gain the initial data. The simulation scenarios differ from each other based on the variations of the height, radius, and tube radius of the Corona ring. After gaining the data, they are divided into three training, validation, and test subsets. By using the training and validation dataset, the proposed model guarantees the high accuracy of the model, then, in the test phase, the data out of the training/validation range are used to test the performance of the model.

2. Finite Element Modelling for Calculating the Electrical Field in Insulators

To solve the problem of electric field calculation imposed on the insulator and Corona ring, the Finite Element Method (FEM) is used to create the data set for the AI-based surrogate models. FEM was firstly introduced in 1960s and was applied in electromagnetic problems in 1965. These days, FEM is a tool in electrical engineering that is used as major numerical method for characterizing the insulator under electro-magnetic fields (Subba Reddy *et al.*, 2010). Generally, FEM includes discretizing the understudied domain into finite numbers of elements, determining the governing equations for each element, and then solving these equations for these elements. Usually, this is conducted by imposing the boundary and initial condition of the problem. For this purpose, the first step is to recognize the equations applied to the problem. Equations (1) to (4) demonstrated the Maxwell equations applied to the electrical field calculation problem (Seyyed Meysam Seyyed Barzegar, et al, 2021).

$$\nabla \times E = \frac{\partial B}{\partial t} \quad (1)$$

$$\nabla \times H = J + \frac{\partial D}{\partial t} \quad (2)$$

$$\nabla . B = 0 \quad (3)$$

$$\nabla . B = \rho \quad (4)$$

where E is the electrical field, B is the magnetic field, H is the intensity of the magnetic field, J is the current density, ρ is the density of electrical charges, and D is the density of electrical flux. After understanding the equations regarding the electrical field calculations, the next step is to conceive the geometry of the insulator as well as the geometry of the Corona ring (Seyyed Meysam Seyyed Barzegar, et al, 2021).

In other words, a 2D electrostatic problem is applied to the insulator problem aiming to find the electric potential distribution. For this purpose, the above equations, could be rewritten as equations (5) to (8), to gain the electric potential distribution (Subba Reddy *et al.*, 2010).

$$\frac{\partial^2 \varphi}{\partial x^2} + \frac{\partial^2 \varphi}{\partial y^2} = 0 \quad (5)$$

$$\varphi_{S_0} = \varphi_0 \quad (6)$$

$$\varphi_1 = \varphi_2 \, , \varepsilon_1 \frac{\partial \varphi_1}{\partial n} = \varepsilon_2 \frac{\partial \varphi_2}{\partial n} \quad (7)$$

$$\iint \frac{\partial \varphi}{\partial n} \partial s = 0 \, , \varphi_{S_i} = \varphi_i \quad (8)$$

where, φ is the electrical potential, equation (6) shows the potential boundary condition, equation (7) is the boundary condition on the interface of different mediums, equation (8) the is floating potential boundary, and φ_0 is the voltage of the line.

Figure 2 shows the ceramic insulator used in 120 kV high voltage lines with any Corona ring. The top side of the insulator is connected to the tower side and the bottom part is in direct contact with the phase wire. The Corona ring is also connected to the phase wire to redistribute the electrical field imposed on the insulator.

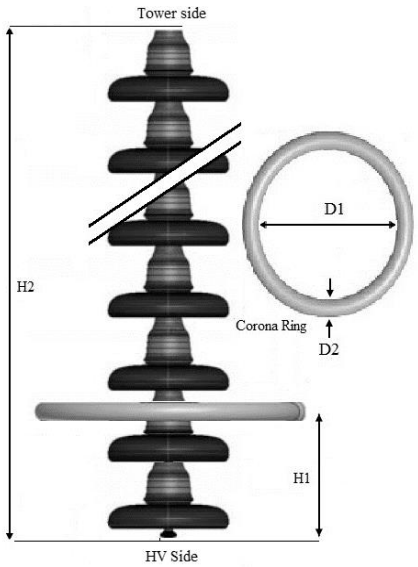

Figure 2. The geometrical presentation of the ceramic insulator and Corona ring (Seyyed Meysam Seyyed Barzegar, et al, 2021)

Table 1. The geometry specifications of the ceramic insulator

Parameter	Definition
D1 (mm)	The outer diameter of the Corona ring
D2 (mm)	tube diameter of Corona ring
R (mm)	Radius of ceramic insulators
H2 (mm)	Height of insulator ring
H1 (mm)	Height of Corona ring

The geometrical parameters of the insulator model are tabulated in Table 1 by considering that the material used for the Corona ring is the same conductor of phase wires and the voltage applied to the end of the insulator is the RMS value of 120 kV high voltage overhead line. The radius of the insulators is 180 mm, the diameter of the caps is approximately 160 mm, the height of the insulator ring is 1696 mm, and the leakage distance is 5510 mm.

3. AI Surrogate Models

A surrogate model is an approximate model/representation of a more intricate or computationally demanding system (Yazdani-Asrami *et al.*, 2023). It comes into play when it's not feasible or dramatically time-consuming to directly model the actual target system. The primary objective of surrogate models is to closely imitate the behavior or outcomes of the target system while maintaining computational efficiency (Tahkola *et al.*, 2020), as shown in Figure 3. These surrogate models find applications in a variety of fields, including optimization, simulation, estimation, and managing uncertainty (Yazdani-Asrami, *et al.*, 2022). As the computation time of FEM-based simulations is very high and for every single change in the characteristics of the Corona ring the whole model should be run again, the surrogate model can be a proper answer to address this drawback of the FEM method. Although AI-based models require an initial data set, once they are trained, they can be used for designing or modelling the system. However, one could argue that due to changes in operational conditions, structural variations, etc. the pre-trained AI models are no longer applicable. In this regard, it should be stated that, unlike static learning, AI models with dynamic learning could be used for considering any changes. Here, static learning means that once the training phase is over, no new data set can be fed into the AI model. Dynamic learning means that new data sets could constantly be fed into the intelligent surrogate model. In this manner, the AI model would upgrade its training hyperparameters to cope with the new data sets. In that way, if a surrogate model gets fed enough input data using the FEM simulations or even real-world sensors, it can predict the maximum electric field that exposes from the system in a very short time and only based on the behavior of the dataset, not its fundamental equations. A surrogate model can be developed based on mathematical formulas, statistical approaches, or AI-based techniques. In this paper, these models have been made using Artificial Intelligence techniques. There are some types of machine learning methods that the models have been developed and used based on them. In this paper, the models that can be used in the regression problems have been implemented. During this section, the architecture of the methods that have been used in this paper will be explained.

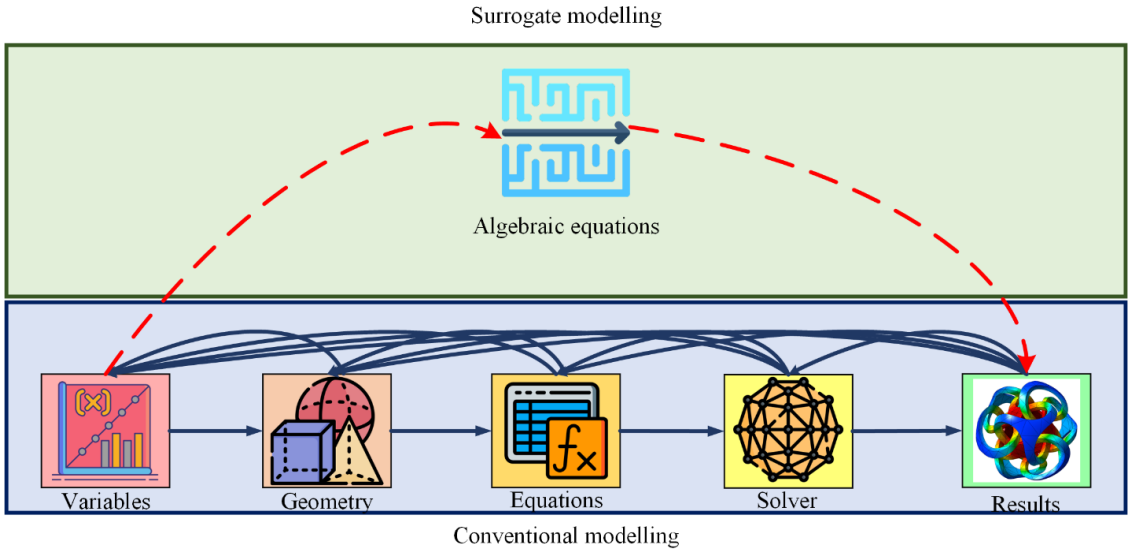

Figure 3. A general overview of the concept of surrogate modelling

It should be noted that insulators operate in different environmental conditions such as pollution, ice, water droplets, etc. Under such circumstances, the delivered AI-based surrogate model could be used employing dynamic learning where different parameters of environmental conditions such as humidity level, pollution level, temperature, etc. could be fed into the AI model. In this stage, the AI-based model with dynamic learning could upgrade itself to cope with the environmental changes of insulators and corona rings. On the other hand, the provided surrogate model aims to characterize the impact of the corona ring on the electric field distribution of the insulator, in clean conditions. This is conducted to design the corona ring, before installing of insulator in a real-world power system.

3.1. Cascade Forward Neural Network

CFNN is a type of neural network that has been developed based on the Feed-Forward Neural Network (FFNN). In the FFNN, the model has multiple layers including input, hidden, and output layers, each one with an independent number of neurons. The input layer takes in electric field attributes, which in this paper, are the geometrical parameters of the ceramic insulator. In the intermediate layers, which can vary in quantity and size (the number of neurons), mathematical operations are performed on the input data using weighted connections. Each neuron within these intermediate layers applies a non-linear activation function to its weighted inputs, allowing the network to capture complex relationships and non-linear patterns in the data. The final layer produces an estimated electric field based on the computations carried out in the previous layers. The CFNN stands out from other Artificial Neural Network (ANN) variants due to its distinctive sequential learning method. In contrast to FFNN, where data passes through the layers in a single step, CFNN employs a two-step learning approach. In the initial stage, a hidden layer is trained using a conventional feed-forward learning algorithm (Alkhasawneh et al, 2018; Alzayed, et al, 2021; Ituabhor *et al.*, 2022). Subsequently, in the second stage, additional hidden units are incrementally added in a cascading manner, with each unit being trained to minimize the remaining error from the preceding layer. This sequential learning process enables the network to progressively refine its estimations layer by layer, leading to an incremental improvement in accuracy and an enhancement in the overall estimation performance. The CFNN is different from the FFNN because it gradually adds more weight factors in each layer which has been indicated in Figure 4. This means that as you go deeper into the layers of the CFNN, more factors affect the result, considering the outputs from all the previous layers whilst in the FFNN, only one factor from

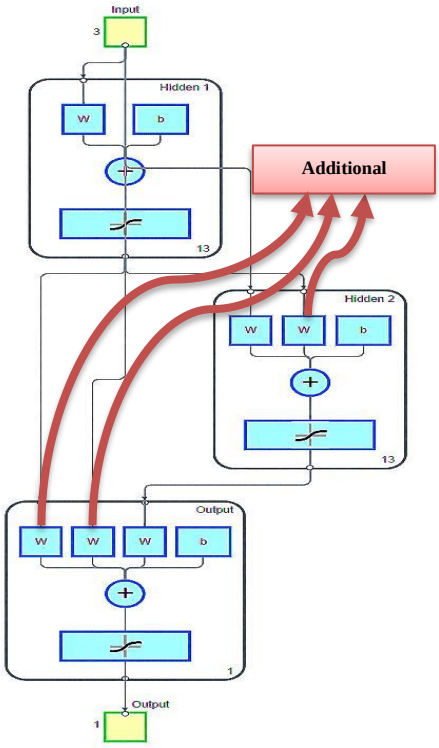

Figure 4. Schematic of the CFNN method

the previous layer affects the result, not all the previous ones. This helps CFNN learn complex patterns in a step-by-step way, making it better at understanding intricate patterns and performing well (Alkhasawneh, 2019; Mohammadi *et al.*, 2021).

The related mathematical equation for CFNN can be expressed as equation (9) (Ituabhor *et al.*, 2022):

$$y_p = \sum_{i=1}^{n} g^i w_i^0 x^i + g^0 \left(\sum_{j=1}^{n} w_i^0 x^i \, g_j^H \left(\sum_{i=1}^{n} w_{jh}^H x_i \right) \right) \quad (9)$$

where g^i and g_j^H designate the output layer and the hidden layer activation functions, respectively. By adding bias to both the input layer and the hidden layers, equation (9) can be modified to equation (10) (Ituabhor *et al.*, 2022):

$$y_p = \sum_{i=1}^{n} g^i w_i^0 x^i + g^0 \left(w^b + \sum_{j=1}^{n} w_i^0 x^i g_j^H \left(w_i^0 + \sum_{i=1}^{n} w_{jh}^H x_i \right) \right) \quad (10)$$

where w_j^H and w^b indicate the respective weight from bias to the hidden layer and output layer.

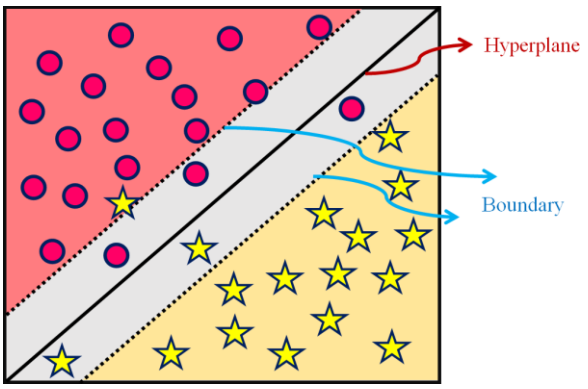

Figure 5. A general presentation of SVR methods which is used to make a regression between two types of data.

3.2. Support Vector Regression

SVR is a well-known technique of machine learning that is widely used by researchers in science and engineering for regression and classification problems. It was developed based on the Support Vector Machine (SVM) algorithm which is a powerful tool for classification problems.

According to what is shown in Figure 5, generally, SVR tries to generate new data using the input dataset to transfer the given data into a high-dimensional space. Then, it implements a simple linear regression method to fit a line to the dataset. Finally, the goal is to find the optimal hyperplane in an N-dimensional space that is positioned to capture the greatest number of data points (Chen *et al.*, 2023). The non-linear data can be represented by a fitting equation which is formulated and is as follows:

$$f(x) = w^{v}\varphi(x) + b \tag{11}$$

In equation 7, w represents the weight factor, and φ is the function employed by SVR to transform the input data into a higher-dimensional space. This transformation helps establish stronger relationships between variables and minimizes errors in the model. The mathematical formulation that SVR tries to minimize errors is as follows (Vapnik, 2000; Li et al, 2023):

$$Objective\ function: \left[\frac{||w||^2}{2} + U\left(v\epsilon + \frac{1}{K}\sum_{i=1}^{K}(\zeta_i, \zeta_i^*)\right)\right] \tag{12}$$

In these equations, $\frac{||w||^2}{2}$ is the regularization factor, U is cost function for model's smoothness balancing and ϵ is loss function, v is a controller varying from 0 to 1 to control the number of support vectors, ζ_i, ζ_i^* are non-negative slack parameters, and K is the number of observations of the training dataset. More details regarding this technique can be found (Li *et al.*, 2023; Zheng *et al.*, 2023).

The equation to evaluate ω can be expressed as follows:

$$\omega = \Sigma_{i=1}^{K}(\alpha_i^* - \alpha_i)\phi(x_i) \tag{13}$$

In equation (13), the terms α_i^* and α_i are Lagrange multipliers. By defining the kernel function of the SVR as equation (14), equation (11) can be rewritten as equation (15) (Liu *et al.*, 2023):

$$U(x_i, x_j) = \phi(x_i)^T\phi(x_j) \tag{14}$$

$$f(x) = \Sigma_{i=1}^{n}(\alpha_i^* - \alpha_i)\, U(x_i, x_j) + b \tag{15}$$

3.3. K-Nearest Neighbors Regression

KNN is a machine learning technique that employs a straightforward logic for estimating the value of a new data point based on its proximity to a set of K-nearest training data points. In other words, the model functions by calculating the distance between a new observation and all the adjacent existing observations in the training dataset (Keramat-Jahromi *et al.*, 2021).

One critical aspect of KNN is the choice of distance metric. There are various ways to evaluate the distance between the data points, namely Manhattan Distance, Minkowski Distance, etc. (Zhang *et al.*, 2023). In this study, the Euclidean distance metric is employed for this purpose, which is very common among those researchers who use KNN, and its mathematical equation has been expressed in equation (16):

$$\text{Euclidean: } d(x_i, x_j) = \sqrt{\Sigma_{k=1}^{p}(x_{ik} - x_{jk})^2}$$

$$\text{Manhattan: } d(x_i.x_j) = \Sigma_{i=1}^{p}|x_{ik} - x_{jk}| \tag{16}$$

$$\text{Minkowski: } d(x_i\ x_j) = \left(\Sigma_{i=1}^{p}|x_{ik} - x_{jk}|^n\right)^{\frac{1}{n}}$$

In this equation, p is the number of input features, x_{ik} is the value of k^{th} input feature for the i^{th} observation, and n is the power parameter which often set to 2. After calculating the distances for all neighboring data points, the algorithm proceeds to select the K neighbors with the lowest distances to the new data point. This set of K-nearest neighbors is crucial for making predictions. In the case of classification, it can be used to determine the majority class among these neighbors.

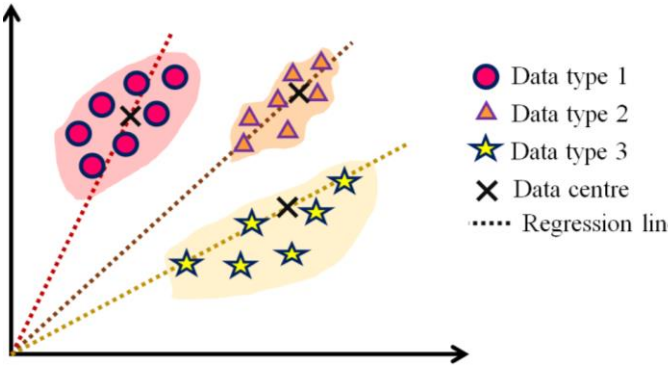

Figure 6. A general presentation of KNN method which is used to make a regression between 3 types of data.

For regression tasks, the mean value of these K-nearest data points is considered as the prediction value, making KNN a powerful tool for both classification and regression problems. Furthermore, it's important to note that the choice of the value 'K' is a hyperparameter that can significantly impact the model's performance. Then, the mean value of the selected points will be considered as the prediction value (Keramat-Jahromi *et al.*, 2021). Further details regarding this method can be found on (Keramat-Jahromi *et al.*, 2021). A general overview of the KNN method is shown in Figure 6.

In addition, it is very common to standardize the dataset for the KNN method before the modelling. In this study, the standard scaling technique has been used which its mathematical equation can be expressed as equation (17):

$$x_i' = \frac{x_i - \bar{x}}{Std} \tag{17}$$

where x_i' is the standardized value of x_i, $\bar{x}$ is the mean value of x parameter, and std is the standard deviation of x parameter which can be expressed as equation (22).

3.4. Performance indexes

To assess the model's accuracy, making comparison between them, and reaching the optimum setup of AI surrogate model, some indexes should be considered to indicate the performance of estimation in a numerical manner. There are various options for these indexes which can be used for data analysis. The indexes used in this paper have been chosen according to the popularity of among researchers and data scientists in recent years (Yazdani-Asrami, *et al.*, 2022; Wu, et al, 2023):

$$RMSE = \sqrt{\sum_{k=1}^{n_s} \frac{(t_k - y_k)^2}{n_s}} \tag{18}$$

$$R^2 = \frac{\sum_{k=1}^{n_s}(t_k - \underline{t})\left(y_k - \underline{y}\right)}{\sqrt{\sum_{k=1}^{n_s}(t_k - \underline{t})^2 \sum_{k=1}^{n_s}\left(y_k - \underline{y}\right)^2}} \tag{19}$$

$$MAE = \sum_{k=1}^{n_s} \frac{|t_k - y_k|}{n_s} \tag{20}$$

$$MARE = \sum_{k=1}^{n_s} \frac{\left|\frac{(t_k - y_k)}{y_k}\right|}{n_s} * 100 \tag{21}$$

$$Std = \sqrt{\frac{\sum_{k=1}^{m}\left(\underline{y} - y_k\right)^2}{m-1}} \tag{22}$$

In equations (18)-(22), y is the predicted value, $\underline{y}$ is mean value of y in m iterations, n_s is the number of samples of the training dataset, t_k is the actual value (target value), and $\underline{t_k}$ is the mean value of t_k.

4. Results and Discussions

4.1 Results of FEM-based simulation

The results of the FEM-based simulations, using COMSOL simulation software, are shown in Figure 7 where Figure 7(a) and Figure 7(b) show the electric potential distribution on the ceramic insulator in absence and presence of the Corona ring, respectively and the arrows in these two figures represent the electrical field. In the presence of the Corona ring the electric field is reduced, compared to the ceramic insulator without Corona ring. In addition, Figure 7(c) of the paper displays the electric field distribution of the insulator without corona ring while Figure 7(d) shows the impact of the Corona ring on the electric field.

Figure 8 shows the impact of adding Corona ring to the structure of the insulator while electric field is considered through the length of the insulator. Based on this figure, the maximum electric field is 32% reduced when Corona ring is added to the insulator. As a result of this field reduction, the life of insulator would be increased and thus, the insulators flashover would be imposed to the power system.

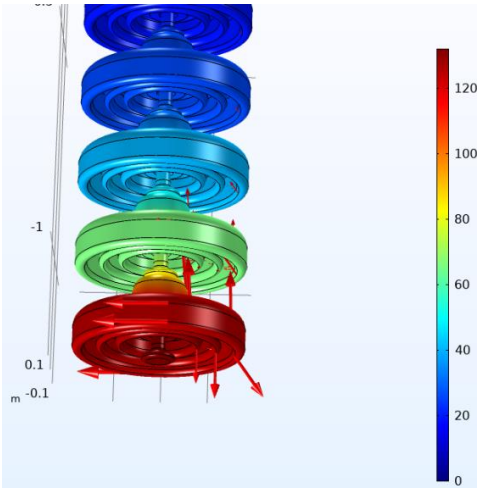

a) Electrical potential without Corona ring

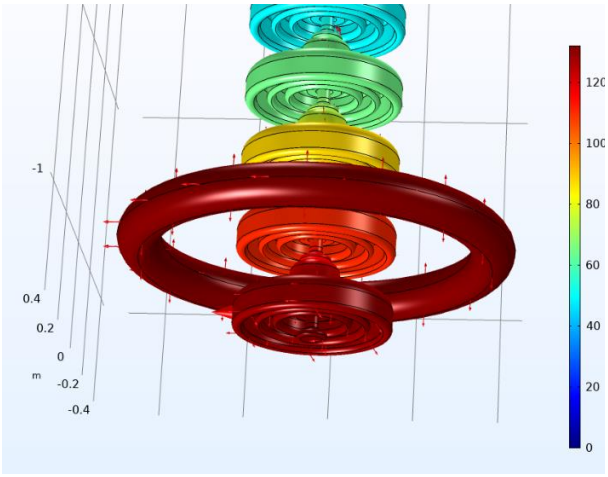

b) Electrical potential with Corona ring

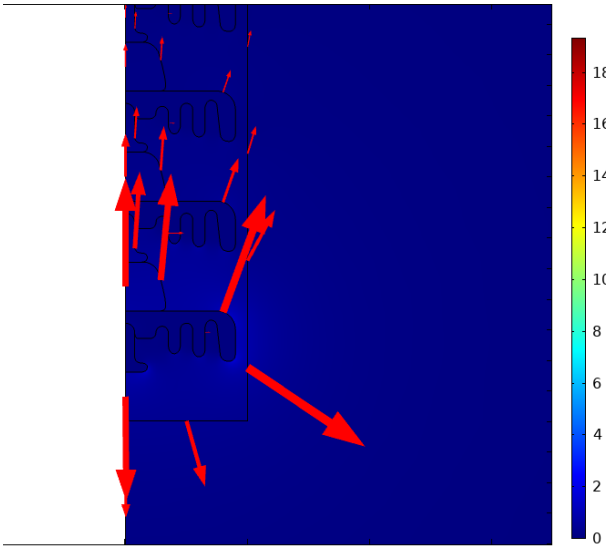

c) Electrical field without Corona ring

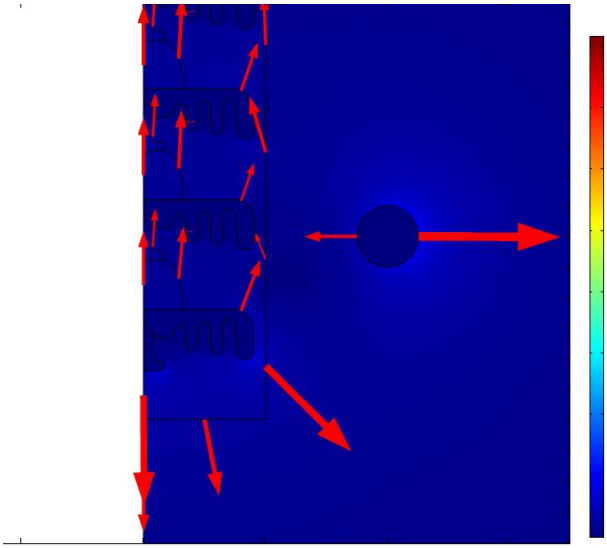

d) Electrical field with Corona ring

Figure 7. Electrical potential distribution and electric field distribution of the understudied insulator, based on COMSOL simulation software

4.2. Data preprocessing

Data collection and preprocessing is of paramount importance in any machine-learning modelling process. Without an appropriate input dataset, the model will not result in high-accuracy prediction. In this paper, as it was discussed in section 2, the input dataset will be collected using the results of the FEM modelling. There are three geometrical parameters of the Corona ring, which are corona ring radius, height, and internal radius. Then, these inputs are used to model the maximum electrical field on the body of the insulator. For this purpose, FEM-based simulations have been performed, and the maximum electric field that is radiated on the surface of the conductor is extracted from the simulations which is used as the target parameter for the AI-based surrogate models. Then, these data are well organized in a tabular mode, making it suitable for implementation in all the three mentioned AI surrogate models. Finally, the dataset will be divided into two different datasets in a random manner, each of them for use for training and testing of the AI models. Although the ratio of this purpose is very dependent on the dataset in every AI modelling, most of the researchers choose a ratio of 70% to 90%. In this study, 70% of the initial dataset is chosen for the training step, meaning that the model will be trained with 700 data points and tested with 300 remaining ones, this is to ensure that the model is well trained while avoiding the risk of overfitting. It should be noted that, Although the selection of the Corona ring design parameters could be affected by cost and weight factors, the most important aspect of

Corona ring is structural design parameters as they have been discussed in this paper.

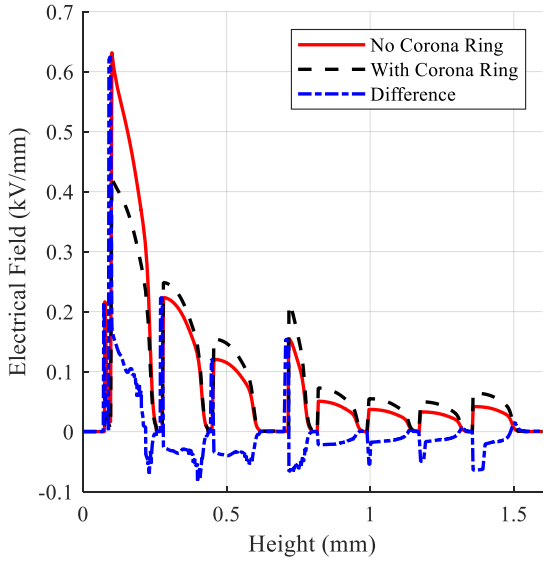

a) Electric field distribution on the edge of the caps

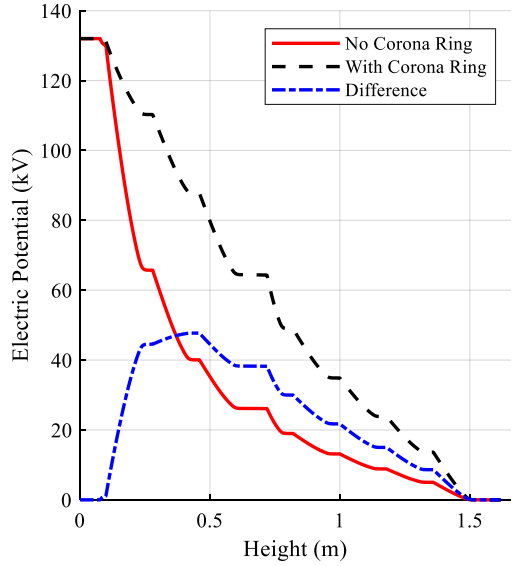

b) Electric potential distribution on the edge of the caps

Figure 8. Electrical field distribution in the presence and absence of the Corona ring, based on COMSOL simulation software

4.3 Simulation data set

As was discussed in section 4.2, three main variables for the design of corona ring are its radius, height, and internal radius. For the purposes of this investigation, it is considered that these parameters vary between 0.2 m - 0.3 m for the radius, 0.8 m - 1.3 m for the height, and 0.005 m - 0.035 m for the internal radius. Then, each period has been divided into 10 values to check the effect of the change of each parameter more concisely. Therefore, a dataset with a total number of 1000 configurations for the corona ring have been made for the training and testing process. The input dataset needs to be used in a tabular format for the AI model. That said, in terms of the illustration of the input dataset here, a 4D figure (3-dimenssional figure with color coding), each nominating for one of the mentioned parameters. As it can be seen with the Figure 9, the maximum electric field is varying significantly with different configurations of the corona ring from 0.5 kV/mm to more than 4 kV/mm. For the purposes of simulation and developing the surrogate model, this dataset will be used as input for the formulas that was discussed in section 3-1, 3-2, and 3-3 to result in the predicted electric field of each configuration. This process is also known as an epoch. After each epoch, the model compares the new results with those from the previous epoch and checks if the trend of the simulation epochs is converging. This process will continue until the error between two epochs reaches a certain level or becomes steady (with negligible changes between epochs). Finally, the trained model must be tested with the test portion of the dataset.

4.4. Comparison between results of different methods

To make the understanding of the process easier, in this section, the overall accuracy of different AI surrogate models will be represented. As can be seen in Table 2, the CFNN model has the highest accuracy in terms of R-squared with 0.998096. Also, regarding the RMSE column, CFNN has almost a quarter RMSE value of the KNNR and almost 40% better accuracy than SVR. On the other hand, the MAE and MARE of CFNN are extensively lower than other models. As a substitute choice for the CFNN model, SVR with an R-squared value of 94.37% can serve as a model with moderate accuracy and a reasonable training time. On the other hand, KNNR, while having the lowest accuracy among these three options at 67.26% R-squared, compensates by being the quickest in terms of training time, taking just 0.019 seconds to be trained. This is considerably faster than CFNN and SVR, which require 3.901 and 0.741 seconds, respectively. This means that although the CFNN model is by far more accurate, it demands more time to get trained with data. That said, the main parameter that is very important is the testing time in which the user can get the electric field intensity. Therefore, after the training process, the response time of trained models to new data points were measured. While the testing time never exceeded 67 ms at the worst, the time is still significantly lower than FEM simulation which takes more than 18 seconds to evaluate the electric field of only one condition.

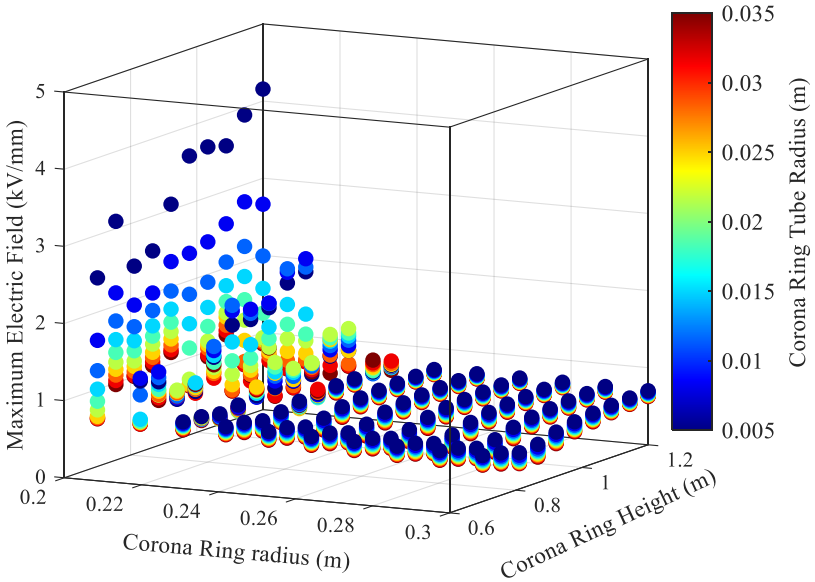

Figure 9. Distribution of data used in this paper for surrogate modelling of the insulator in presence of the Corona ring

It is worth noting that the nature of different programming languages affects the reported time as the CFNN model has been developed on MATLAB 2023b software whilst the SVR and KNNR methods have been on Python version 3.11.5. Also, the operating system during this process remained the same, which has an 11th Gen Intel(R) Core (TM) i5-1135G7 CPU and 8.00 GB RAM.

Table 2. Comparison of performance of different AI surrogate models based on different metrics.[1]

Method	RMSE [kV/mm]	R^2	MAE	MARE [%]	Training time [s]	Testing time [ms]
CFNN	**0.0454**	**0.998**	**0.011**	**0.152**	**3.901**	**7.432**
SVR	0.0849	0.943	0.041	4.742	0.741	67.118
KNNR	0.204	0.672	0.070	7.542	0.019	13.238

4.5. Sensitivity Analysis

A necessary step for AI modeling is the sensitivity analysis of effective parameters on the model's accuracy. This process, which is also known as hyperparameter tuning, will increase the robustness and accuracy of the final model. There is no predefined setup of these parameters that can result in the highest accuracy for all datasets and so they need to be tested and compared to reach the optimum choice. As the CFNN was the best model amongst the three proposed ones, in the following, the procedure of the sensitivity analysis will be focused and explained for CFNN and only the optimum (best) hyperparameters of the other methods will be reported.

One of the most effective parameters on the CFNN model performance is the number of hidden layers as they play a crucial role in the accuracy and the predictability of the model. Many researchers use a single-layer model which is simpler and requires less training time compared with multi-layer choices. That said, single-layer models are less accurate than multilayer models in most cases. Therefore, an analysis of the number of hidden layers is done in this paper and the results can be found in Figure 10, Figure 11, and Table 3.

As it appears from Figure 10, in terms of RMSE which is illustrated with the green dots and line, the quintuple model with 0.0455 has the lowest error which is almost half of the single layer model. Also, regarding the R-squared index, which has been demonstrated with the red line, the quintuple model has the highest value that means the model is well-trained and has extensively high accuracy in prediction of the real values. Furthermore, after training of the model, they are tested with all the input dataset and the response time is measured and reported in Figure 11. As it is clear, the model with 5 layers has a relatively higher response time in comparison with other conditions. That said, considering that all the testing time is in millisecond scale and has been tested on personal computers (instead of powerful high Graphics processing unit computers), we choose 5 layers configuration due to its very high accuracy.

The second extensive important parameter of the CFNN model is the number of neurons in each layer. In this paper, the number of neurons in each layer is considered to vary between 1 to 15, which means that if the number of hidden layers is k, then the

[1] Bold data are chosen as the best scenario.

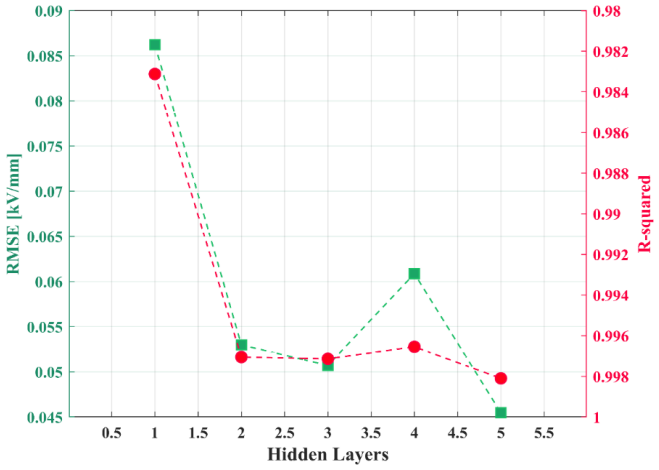

Figure 10. Performance of the CFNN model with different numbers of hidden layers

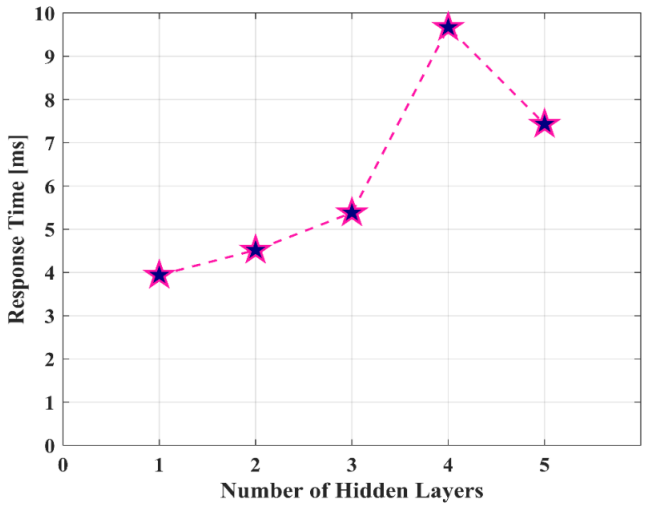

Figure 11. Testing time variation for the CFNN model with different number of hidden layers

total number of cases that are studied as part of sensitivity analysis will be 15^k. This means that since k varies between 1 and 5, a total number of 813615 different conditions has been tested to ensure that the best setup of neurons and hidden layers has been chosen for the model. It is worth noting that each setup has been tested 20 times and then the mean value of each index has been reported. As can be seen in Table 3, the setup with [3 15 7 11 7] configuration of neurons for the quintuple hidden layers model resulted in the highest accuracy amongst all possible setups in terms of both RMSE and R-squared indexes.

Another important parameter that has severe effects on the accuracy of the model is the training function (also called the optimization function). There are various algorithms that have been proposed in literature for the training function. These algorithms are used to minimize the error between the real and the predicted target values, which in this case is an electric field. This aim is done by updating the weight and bias factors after every epoch. An epoch refers to one complete pass through the entire training dataset. During each epoch, the model is exposed to the entire training dataset, and the model's parameters are updated based on the error (or loss) it incurs, with the goal of improving its performance on the task it's being trained for. As this updating process can also be in the direction of dropping the accuracy of the model, a goal parameter for the number of consecutive epochs that worsen the accuracy should be made, which in this work has been set to 20.

Table 3. Performance of the CFNN model by considering the best setup of neurons for each number of layers[2]

Hidden Layers	Neurons	RMSE [kV/mm]	R^2	Testing time [ms]
1	13	0.0862	0.9831	3.9392
2	[13 13]	0.0529	0.9970	4.5176
3	[5 11 15]	0.0507	0.9971	5.3823
4	[15 11 3 7]	0.0608	0.9965	9.6705
5	**[3 15 7 11 7]**	**0.0454**	**0.9980**	**7.4320**

Table 4. Performance of CFNN model using different training functions[3]

Training Function	RMSE [kv/mm]	R^2	Time [ms]
LM	**0.0454**	**0.9980**	**7.4320**
SCG	0.0973	0.9808	14.6171
RB	0.1004	0.9798	12.6820
VLRB	0.2006	0.9300	12.6203

In this paper, four of the existing algorithms that are used in namely (Yazdani-Asrami, Sadeghi, Seyyedbarzegar, *et al.*, 2022; Alipour Bonab, Song and Yazdani-Asrami, 2023) Levenberg–Marquardt (LM), Scaled Conjugate Gradient (SCG), Resilient Backpropagation (RB), and Variable Learning Rate Backpropagation (VLRB), have been tested. Then, a comprehensive comparison between the accuracy of the models based on these algorithms has been demonstrated in Table 4. As can be seen with Table 4, the model that uses LM as training

[2] Bold data are chosen as the best scenario.

[3] Bold data are chosen as the best scenario.

function has the highest accuracy and lowest response time at the same time.

The other effective parameter that has a huge impact on the accuracy of the final model is the Activation function. Its primary purpose is to introduce non-linearity into the network, allowing it to learn complex patterns and relationships in the data by transforming the weighted sum of inputs into a non-linear output. Activation functions are responsible for deciding the activation state of a neuron according to its input. When the input surpasses a particular threshold, the neuron becomes active, resulting in a non-zero output. Conversely, if the input does not meet this threshold, the neuron remains inactive, yielding an output of zero. In this paper, the sensitivity analysis phase includes the evaluation of four activation functions, namely purelin, tansig, satlin, and logsig. These functions have been chosen due to their widespread use in the existing literature (Yazdani-Asrami, *et al.*, 2022) and their mathematical equation has been provided in equations (23) to (26). Moreover, to make it easier to compare their mathematical functions, these activation functions have been illustrated in Figure 12.

Pure linear:

$$a(x) = x \tag{23}$$

Saturated linear:

$$a(x) = \{0 \quad x < 0 \; x \quad 0 < x < 1 \; 1 \quad x > 1 \tag{24}$$

Hyperbolic tangent sigmoid:

$$a(x) = tanh(x) \tag{25}$$

Log–sigmoid;

$$a(x) = \frac{1}{1 + exp(-x)} \tag{26}$$

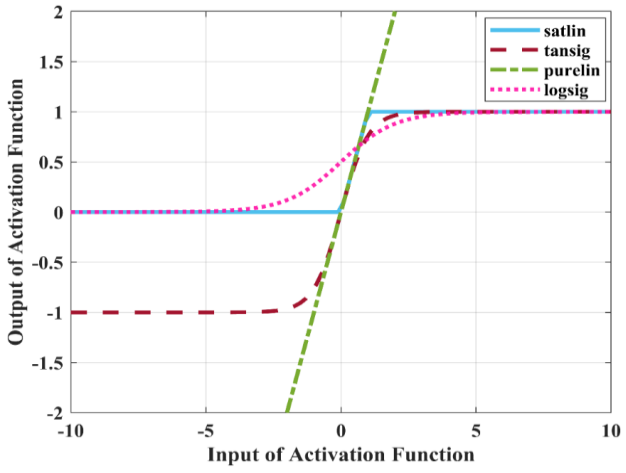

Figure 12. A schematic of different activation functions in this work

In this paper, 8 pairs out of all possible pairs have been tested, and the results are shown in Table 5. As can be seen with Table 5, the Tansig-Purelin pair has the highest performance as it has the lowest RMSE while the highest R-squared. This means that it implements tansig as the activation function between the input layer and the hidden layers, and between two hidden layers while using purelin as the activation function between the last hidden layer and output layer.

Table 5. Performance of the CFNN model by using different pairs of activation functions[4]

Pair of activation functions	RMSE [kV/mm]	R^2
Purelin-Tansig	0.2185	0.8465
Tansig-Purelin	**0.0454**	**0.9980**
Satlin-Tansig	0.0901	0.9867
Tansig-Satlin	1.5767	0.2696
Purelin-Logsig	1.5663	0.4006
Logsig-Purelin	0.0589	0.9968
Satlin-Logsig	1.5629	0.16513
Logsig-Satlin	1.5655	0.4760

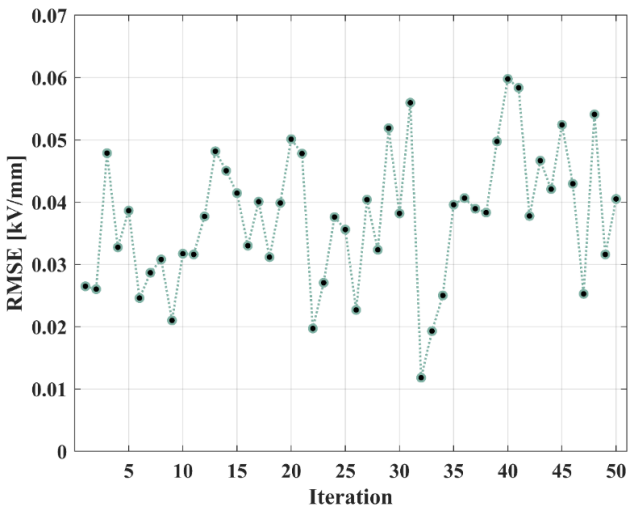

Figure 13. Stability analysis for the final setup

After finishing the sensitivity analysis, the final model which has five hidden layers, a setup of neuron [**3 15 7 11 7**], LM as the training function, and Tansig-Purelin as the pair of activation functions needs to be tested to ensure that the model is stable. A valuable index that can help us in this step is standard deviation which was proposed in equation (22). In this work, considering random splitting of data, the training of the final model regarding the results of the previous steps, has been repeated 50 times and the RMSE for each iteration is indicated in Figure 13. Also, using the standard deviation of these values

[4] Bold data are chosen as the best scenario.

is 0.01091 which demonstrates that the model is considered as stable setup.

To summarize the findings of the explained sensitivity analysis, the best setup for the CFNN model along with the SVR and KNNR models are mentioned in Table 6.

Table 6. Hyperparameter for all three methods

Method	CFNN	SVR	KNNR
Hyperparameter	number of layers=3 number of neurons=15 training function= Levenburg-Marquardt activation_function = Tansig - Purelin	kernel='g' C=100 epsilon=0.01 degree=3 gamma='scale'	n_neighbors=10 weights='uniform' algorithm='auto' leaf_size=30 p=2

5. Conclusion

The Corona ring is used to change the distribution of electric field on the ceramic insulator by connecting it directly to the power line. Usually and based on literature, Corona ring designed through an iterative optimization method parallel with Finite Element Method (FEM). Although the performance of FEM-based models is accurate, their simulation time is still challenging. Using FEM for a new geometry of Corona ring always needs a new run, while with CFNN surrogate model you can easily predict any new cases and the modelling process does not need to be repeated. So, in this paper, a novel intelligent surrogate model is proposed which computes the electric field on the ceramic insulators in a few milliseconds.

The results of this paper are as follows:

- The CFNN method is the best AI surrogate model amongst the three options that have been studied in this paper.
- It can predict the maximum electric field that radiates from the system for different geometries of Corona rings in only few milliseconds with significantly high accuracy of 99.81% accuracy in terms of R-squared. This is while for implementing FEM, this time will take 8.73 seconds, which is thousands of times more than what the AI surrogate model demands.
- Also, the AI surrogate model can be updated by retraining with newer geometry results, while the results of FEM model is only one-time used.
- As an alternative option for CFNN model, the SVR model with 94.37% R-squared can be used as a model with moderate accuracy and training time.
- The KNNR model which has the lowest accuracy among these three options with 67.26% R-squared, is in counteract the fastest method with respect to its training time with only 0.019 seconds, extremely faster than CFNN and SVR with 3.901 and 0.741 seconds, respectively.

Acknowledgments

For the purpose of open access, the author(s) has applied a Creative Commons Attribution (CC BY) license to any Author Accepted Manuscript version arising from this submission.

References

Alipour Bonab, S., Song, W. and Yazdani-Asrami, M. (2023) 'A New Intelligent Estimation Method Based on the Cascade-Forward Neural Network for the Electric and Magnetic Fields in the Vicinity of the High Voltage Overhead Transmission Lines', *Applied Sciences*, 13(20), p. 11180. Available at: https://doi.org/10.3390/app132011180.

Alkhasawneh, M.Sh. (2019) 'Hybrid Cascade Forward Neural Network with Elman Neural Network for Disease Prediction', *Arabian Journal for Science and Engineering*, 44(11), pp. 9209–9220. Available at: https://doi.org/10.1007/s13369-019-03829-3.

Alkhasawneh, M.Sh. and Tay, L.T. (2018) 'A Hybrid Intelligent System Integrating the Cascade Forward Neural Network with Elman Neural Network', *Arabian Journal for Science and Engineering*, 43(12), pp. 6737–6749. Available at: https://doi.org/10.1007/s13369-017-2833-3.

Alti, N., Bayadi, A. and Belhouchet, K. (2021) 'Grading ring parameters optimization for 220 kV metal-oxide arrester using 3D-FEM method and bat algorithm', *IET Science, Measurement & Technology*, 15(1), pp. 14–24. Available at: https://doi.org/10.1049/smt2.12002.

Alzayed, M., Chaoui, H. and Farajpour, Y. (2021) 'Maximum Power Tracking for a Wind Energy Conversion System Using Cascade-Forward Neural Networks', *IEEE Transactions on Sustainable Energy*, 12(4), pp. 2367–2377. Available at: https://doi.org/10.1109/TSTE.2021.3094093.

Aramugam, K., Illias, H.A. and Ching, Y.C. (2019) 'Optimisation of corona ring design for composite insulator strings', *COMPEL - The international journal for computation and mathematics in electrical and electronic engineering*, 38(1), pp. 232–246. Available at: https://doi.org/10.1108/COMPEL-04-2018-0165.

Archana, C. and Usha, K. (2021) 'Optimization of Electric Field Distribution Along a 400-kV Composite Insulator', in, pp. 291–302. Available at: https://doi.org/10.1007/978-981-15-7241-8_21.

Aydogmus, Z. (2009) 'A neural network-based estimation of electric fields along high voltage insulators', *Expert Systems with Applications*, 36(4), pp. 8705–8710. Available at: https://doi.org/10.1016/j.eswa.2008.11.030.

Bo Zhang *et al.* (2006) 'Electric field calculation for HV insulators on the head of transmission tower by coupling CSM with BEM', *IEEE Transactions on Magnetics*, 42(4), pp. 543–546. Available at: https://doi.org/10.1109/TMAG.2006.871373.

Bourek, Y., M'Ziou, N. and Benguesmia, H. (2018) 'Prediction of Flashover Voltage of High-Voltage Polluted Insulator Using Artificial Intelligence', *Transactions on Electrical and Electronic Materials*, 19(1), pp. 59–68. Available at: https://doi.org/10.1007/s42341-018-0010-3.

Chen, K. *et al.* (2023) 'Capacity degradation prediction of lithium-ion battery based on artificial bee colony and multi-kernel support vector regression', *Journal of Energy Storage*, 72, p. 108160. Available at: https://doi.org/10.1016/j.est.2023.108160.

Corona ring (no date) *Wikipedia*. Available at: https://en.wikipedia.org/wiki/Corona_ring (Accessed: 10 November 2023).

Diaz-Acevedo, J.A., Escobar, A. and Grisales-Noreña, L.F. (2021) 'Optimization of corona ring for 230 kV polymeric insulator based on finite element method and PSO algorithm', *Electric Power Systems Research*, 201, p. 107521. Available at: https://doi.org/10.1016/j.epsr.2021.107521.

Halloum, M.-R., Subba Reddy, B. and Razouk, Y. (2022) 'Optimization of Corona Ring Design for 400 kV Polymeric Outdoor Insulator', in *2022 IEEE 6th International Conference on Condition Assessment Techniques in Electrical Systems (CATCON)*. IEEE, pp. 156–160. Available at: https://doi.org/10.1109/CATCON56237.2022.10077685.

Hanyu Ye, Clemens, M. and Seifert, J. (2015) 'Dimension Reduction for the Design Optimization of Large Scale High Voltage Devices Using Co-Kriging Surrogate Modeling', *IEEE Transactions on Magnetics*, 51(3), pp. 1–4. Available at: https://doi.org/10.1109/TMAG.2014.2361916.

Ilhan, S., Ozdemir, A. and Ismailoglu, H. (2015) 'Impacts of corona rings on the insulation performance of composite polymer insulator strings', *IEEE Transactions on Dielectrics and Electrical Insulation*, 22(3), pp. 1605–1612. Available at: https://doi.org/10.1109/TDEI.2015.7116356.

Illias, H.A. *et al.* (2021) 'Optimization of Grading Ring Design for Metal Oxide Arrester Using Gravitational Search Algorithm', in *2021 IEEE International Conference on the Properties and Applications of Dielectric Materials (ICPADM)*. IEEE, pp. 13–16. Available at: https://doi.org/10.1109/ICPADM49635.2021.9493910.

Ituabhor, O. *et al.* (2022) 'Cascade Forward Neural Networks-based Adaptive Model for Real-time Adaptive Learning of Stochastic Signal Power Datasets', *International Journal of Computer Network and Information Security*, 14(3), pp. 63–74. Available at: https://doi.org/10.5815/ijcnis.2022.03.05.

Jiang, H. *et al.* (2018) 'Calculation and Optimization of Electric Field of Insulators with Internal Grading Ring', in *2018 IEEE Electrical Insulation Conference (EIC)*. IEEE, pp. 315–318. Available at: https://doi.org/10.1109/EIC.2018.8481051.

Keramat-Jahromi, M. *et al.* (2021) 'Real-time moisture ratio study of drying date fruit chips based on on-line image attributes using kNN and random forest regression methods', *Measurement*, 172, p. 108899. Available at: https://doi.org/10.1016/j.measurement.2020.108899.

Khajavi, M., Bagheri, S. and Shemshadi, A. (2023) 'Optimal design of corona ring in composite insulator considering the effects of tower structure, conductor, hardware and mutual phases', *Electric Power Systems Research*, 223, p. 109686. Available at: https://doi.org/10.1016/j.epsr.2023.109686.

Khodsuz, M. (2022) 'Externally gapped line arrester performance in high voltage transmission line using frequency grounding system: Absorbed energy and expected life assessment', *IET Science, Measurement & Technology*, 16(7), pp. 426–440. Available at: https://doi.org/10.1049/smt2.12116.

Khodsuz, M., Mirzaie, M. and Seyyedbarzegar, S. (2015) 'Metal oxide surge arrester condition monitoring based on analysis of leakage current components', *International Journal of Electrical Power & Energy Systems*, 66, pp. 188–193. Available at: https://doi.org/10.1016/j.ijepes.2014.10.052.

Li, C. and Mei, X. (2023) 'Application of SVR models built with AOA and Chaos mapping for predicting tunnel crown displacement induced by blasting excavation', *Applied Soft Computing*, 147, p. 110808. Available at: https://doi.org/10.1016/j.asoc.2023.110808.

Li, Y. *et al.* (2023) 'A steps-ahead tool wear prediction method based on support vector regression and particle filtering', *Measurement*, 218, p. 113237. Available at: https://doi.org/10.1016/j.measurement.2023.113237.

Liu, H. *et al.* (2023) 'Hybrid prediction model for cold load in large public buildings based on mean residual feedback and improved SVR', *Energy and Buildings*, 294, p. 113229. Available at: https://doi.org/10.1016/j.enbuild.2023.113229.

Maraaba, L., Al-Hamouz, Z. and Al-Duwaish, H. (2014) 'Estimation of high voltage insulator contamination using a combined image processing and artificial neural networks', in *2014 IEEE 8th International Power Engineering and Optimization Conference (PEOCO2014)*. IEEE, pp. 214–219. Available at: https://doi.org/10.1109/PEOCO.2014.6814428.

Maraaba, L., Alhamouz, Z. and Alduwaish, H. (2018) 'A neural network-based estimation of the level of contamination on high-voltage porcelain and glass insulators', *Electrical Engineering*, 100(3), pp. 1545–1554. Available at: https://doi.org/10.1007/s00202-017-0634-z.

Medeiros, A. *et al.* (2022) 'Comparison of artificial intelligence techniques to failure prediction in contaminated insulators based on leakage current', *Journal of Intelligent & Fuzzy Systems*, 42(4), pp. 3285–3298. Available at: https://doi.org/10.3233/JIFS-211126.

M'Hamdi, B. *et al.* (2022) 'Multi-Objective Optimization of 400 kV Composite Insulator Corona Ring Design', *IEEE Access*, 10, pp. 27579–27590. Available at: https://doi.org/10.1109/ACCESS.2022.3157384.

M.M Abravesh, A.S.H.A.M.Y. asrami (2016) 'Estimation of parameters of metal-oxide surge arrester models using Big Bang-Big Crunch and Hybrid Big Bang-Big Crunch algorithms', *Journal of Artificial Intelligence and Data Mining*, 4(2). Available at: https://doi.org/10.5829/idosi.JAIDM.2016.04.02.12.

Mohammadi, M.-R. *et al.* (2021) 'Application of cascade forward neural network and group method of data handling to modeling crude oil pyrolysis during thermal enhanced oil recovery', *Journal of Petroleum Science and Engineering*, 205, p. 108836. Available at: https://doi.org/10.1016/j.petrol.2021.108836.

Niazi, M.T.K. *et al.* (2020) 'Prediction of Critical Flashover Voltage of High Voltage Insulators Leveraging Bootstrap Neural Network', *Electronics*, 9(10), p. 1620. Available at: https://doi.org/10.3390/electronics9101620.

Salhi, R. *et al.* (2023) 'Corona Ring Improvement to Surface Electric Field Stress Mitigation of 400 kV Composite Insulator', *IEEE Transactions on Dielectrics and Electrical Insulation*, pp. 1–1. Available at: https://doi.org/10.1109/TDEI.2023.3342772.

Seyyed Meysam Seyyed Barzegar, Alireza Sadeghi and Masume Khodsuz (2021) 'Optimization of Corona Ring Parameters for Electric Field Adjustment in Composite Insulator Using Derivative Free Solvers', *Computational Intelligence in Electrical Engineering*, 12(1), pp. 75–86.

Seyyedbarzegar, S. and Khodsuz, M. (2021) 'Surge arrester operation investigation in low- and high-current regions using MATLAB GUI: Implementing an educational goal for undergraduate students', *Computer Applications in Engineering Education*, 29(5), pp. 1267–1283. Available at: https://doi.org/10.1002/cae.22384.

Seyyedbarzegar, S.M. and Mirzaie, M. (2015a) 'Application of finite element method for electro-thermal modeling of metal oxide surge arrester', *Computer Applications in Engineering Education*, 23(6), pp. 910–920. Available at: https://doi.org/10.1002/cae.21663.

Seyyedbarzegar, S.M. and Mirzaie, M. (2015b) 'Heat transfer analysis of metal oxide surge arrester under power frequency applied voltage', *Energy*, 93, pp. 141–153. Available at: https://doi.org/10.1016/j.energy.2015.09.031.

Shi, Y. and Wang, Z. (2019) 'Calculating for surface electric field of converter valve shield system with fast multipole curved boundary element method', *The Journal of Engineering*, 2019(16), pp. 1575–1579. Available at: https://doi.org/10.1049/joe.2018.8647.

Subba Reddy, B. *et al.* (2010) 'Simulation of potential and electric field for high voltage ceramic disc insulators', in *2010 5th International Conference on Industrial and Information Systems*. IEEE, pp. 526–531. Available at: https://doi.org/10.1109/ICIINFS.2010.5578647.

Tahkola, M. *et al.* (2020) 'Surrogate Modeling of Electrical Machine Torque Using Artificial Neural Networks', *IEEE Access*, 8, pp. 220027–220045. Available at: https://doi.org/10.1109/ACCESS.2020.3042834.

Vapnik, V.N. (2000) *The Nature of Statistical Learning Theory*. New York, NY: Springer New York. Available at: https://doi.org/10.1007/978-1-4757-3264-1.

Waghmare, V. V., Yadav, V.K. and Desai, I.M. (2022) 'Optimization of Grading Ring of Surge arrester by using FEM method, PSO & BAT Algorithm', in *2022 2nd International Conference on Advance Computing and Innovative Technologies in Engineering (ICACITE)*. IEEE, pp. 367–370. Available at: https://doi.org/10.1109/ICACITE53722.2022.9823652.

Wu, G. and Yong, H. (2023) 'Estimation of critical current density of bulk superconductor with artificial neural network', *Superconductivity*, 7, p. 100055. Available at: https://doi.org/10.1016/j.supcon.2023.100055.

Yazdani-Asrami, M., Sadeghi, A., Song, W., *et al.* (2022) 'Artificial intelligence methods for applied superconductivity: material, design, manufacturing, testing, operation, and condition monitoring', *Superconductor Science and Technology*, 35(12), p. 123001. Available at: https://doi.org/10.1088/1361-6668/ac80d8.

Yazdani-Asrami, M., Sadeghi, A., Seyyedbarzegar, S., *et al.* (2022) 'DC Electro-Magneto-Mechanical Characterization of 2G HTS Tapes for Superconducting Cable in Magnet System Using Artificial Neural Networks', *IEEE Transactions on Applied Superconductivity*, 32(7), pp. 1–10. Available at: https://doi.org/10.1109/TASC.2022.3193782.

Yazdani-Asrami, M. *et al.* (2023) 'Roadmap on artificial intelligence and big data techniques for superconductivity', *Superconductor Science and Technology*, 36(4), p. 043501. Available at: https://doi.org/10.1088/1361-6668/acbb34.

Zhang, C. *et al.* (2023) 'A multi-fault diagnosis method for lithium-ion battery pack using curvilinear Manhattan distance evaluation and voltage difference analysis', *Journal of Energy Storage*, 67, p. 107575. Available at: https://doi.org/10.1016/j.est.2023.107575.

Zhang, S. (2021) 'Optimization of Corona Ring Design Used in UHV Composite Insulator by PSO Algorithm', *Journal of Physics: Conference Series*, 2087(1), p. 012032. Available at: https://doi.org/10.1088/1742-6596/2087/1/012032.

Zheng, Y. *et al.* (2023) 'New ridge regression, artificial neural networks and support vector machine for wind speed prediction', *Advances in Engineering Software*, 179, p. 103426. Available at: https://doi.org/10.1016/j.advengsoft.2023.103426.

Corresponding author – Mohammad Yazdani-Asrami can be contacted at: mohammad.yazdani-asrami@glasgow.ac.uk